

Engineered Networks of Synthetic and Natural Proteins To Control Cell Migration

Evan Mills,[†] Elizabeth Pham,[†] Seema Nagaraj,[†] and Kevin Truong^{*,†,‡}

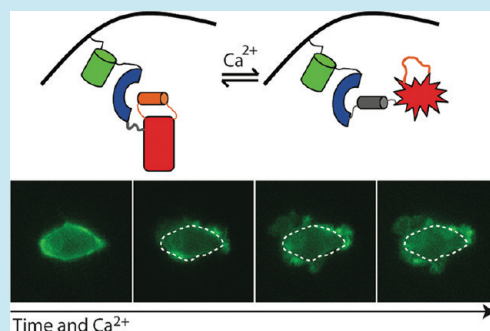
[†]Institute of Biomaterials and Biomedical Engineering, University of Toronto, 164 College Street, Toronto, Ontario M5S 3G9, Canada

[‡]Edward S. Rogers Sr. Department of Electrical and Computer Engineering, University of Toronto, 10 King's College Circle, Toronto, Ontario M5S 3G4, Canada

S Supporting Information

ABSTRACT: Mammalian cells reprogrammed with engineered transgenes have the potential to be useful therapeutic platforms because they can support large genetic networks, can be taken from a host or patient, and perform useful functions such as migration and secretion. Successful engineering of mammalian cells will require the development of modules that can perform well-defined, reliable functions, such as directed cell migration toward a chemical or physical signal. One inherently modular cellular pathway is the Ca^{2+} signaling pathway: protein modules that mobilize and respond to Ca^{2+} are combined across cell types to create complexity. We have designed a chimera of Rac1, a GTPase that controls cell morphology and migration, and calmodulin (CaM), a Ca^{2+} -responsive protein, to control cell migration. The Rac1-CaM chimera (named RACer) controlled lamellipodia growth in response to Ca^{2+} . RACer was combined with LOVS1K (a previously engineered light-sensitive Ca^{2+} -mobilizing module) and cytokine receptors to create protein networks where blue light and growth factors regulated cell morphology and, thereby, cell migration. To show the generalizability of our design, we created a Cdc42-CaM chimera that controls filopodia growth in response to Ca^{2+} . The insights that have been gained into Ca^{2+} signaling and cell migration will allow future work to combine engineered protein systems to enable reprogrammed cell sensing of relevant therapeutic targets *in vivo*.

KEYWORDS: Rac1, calmodulin, LOV2, protein engineering, Ca^{2+}



Novel platforms for therapeutic interventions in humans at the cellular and molecular level include nanoparticles,¹ viruses,² and biomaterials.³ Each class of platform has its particular strengths and weaknesses for a given application; for example, nanoparticles can simultaneously combine multiple modalities such as imaging and payload delivery but are often difficult to target to sites of interest with fidelity, such as a particular cell population within a tumor.¹ Viruses can ensure efficient and reliable transgene delivery to a population of host cells but can have unpredictable consequences on the host such as inflammation and production of viral-neutralizing antibodies.² The use of metazoan cells as a platform for therapeutic application, that is, not simply correcting a genetic defect as is the goal in conventional gene therapy but rather introducing novel function to cells, is a relatively unexplored field. Metazoan cells have several desirable properties as a therapeutic platform including the ability to support large networks of transgenes,⁴ the potential to be drawn from the host or patient themselves,⁵ and the inherent ability to perform useful functions such as migration, secretion, membrane fusion, and target-cell lysis. Some general limitations of metazoan cells as a therapeutic platform are their complexity and heterogeneity, making their overall behaviors often difficult to predict, and stringent handling requirements compared to nanoparticles, viruses or

small-molecule drugs. Notwithstanding these limitations, there are several recent reports in the literature of host or patient metazoan cells being reprogrammed by the delivery of transgenes to perform therapeutically valuable functions *in vivo*, including secreting inflammatory cytokines from tumor cells,² targeting and destruction of chronic lymphocytic leukemia cells by host T-cells,⁵ and expression of RNA-based anti-HIV moieties from hematopoietic stem cells.⁶

Successfully using metazoan cells as therapeutic platforms will require the modular combination of genetic and protein units that can carry out well-defined functions, such as migration, protein secretion, and cell death. Cell migration is a particularly important function because cells will need to migrate from their source (for example, an injection site, the circulation, or bone marrow) to the site of disease or injury. The ability of therapeutically engineered cells to migrate in a predictable way will determine the efficiency and efficacy of a particular strategy and the likelihood of off-target effects. Cell migration is often considered to be under control of the three principal Rho GTPases Rac1, Cdc42, and RhoA.⁷ The simplistic paradigm of the three Rho GTPases is that Cdc42

Received: March 22, 2012

Published: April 28, 2012

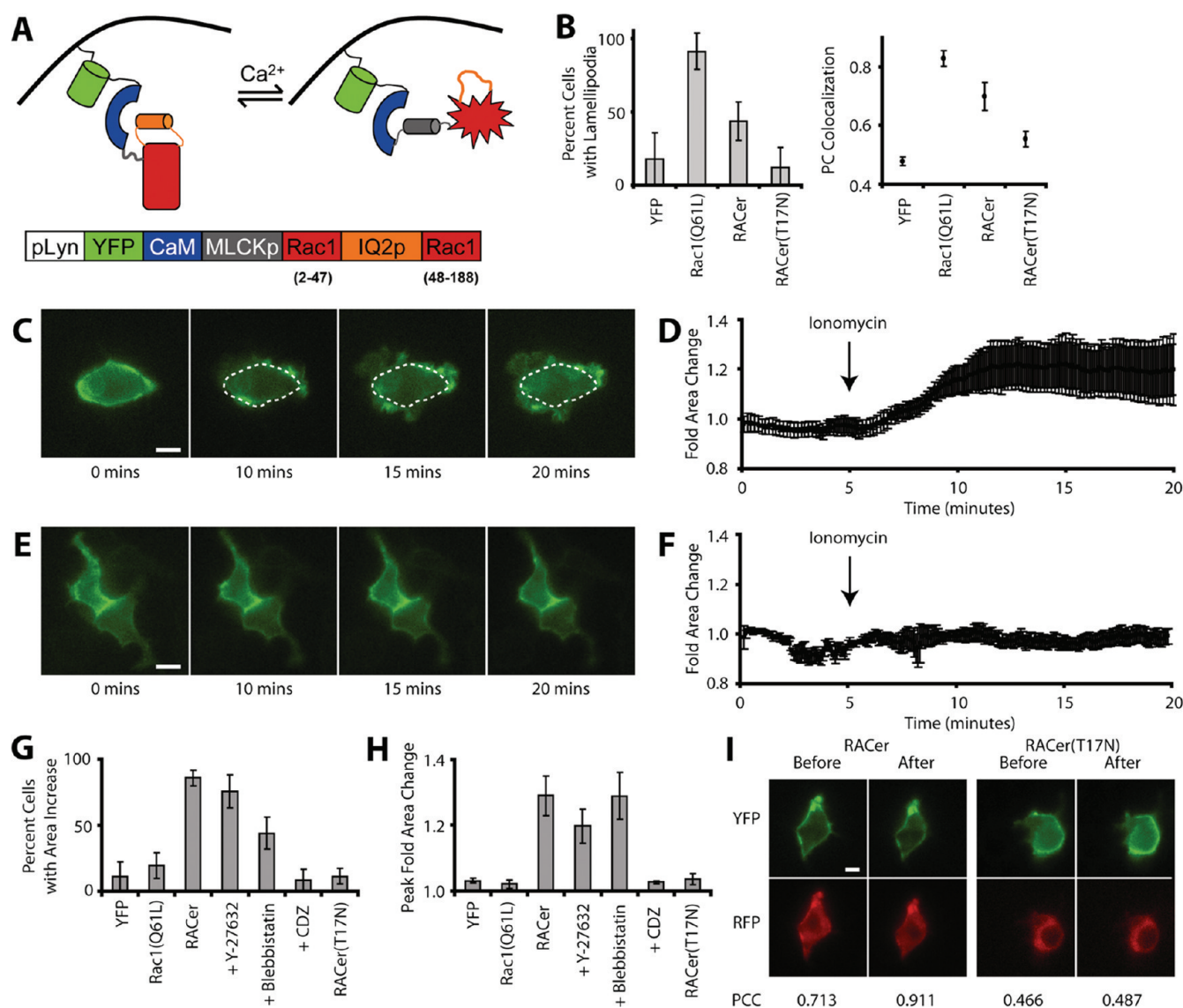


Figure 1. RACer is a Ca^{2+} -activated Rac1-like protein. (A) Cartoon of the binding events in the RACer chimera during Ca^{2+} activation. (B) Analysis of cells before Ca^{2+} stimulation. Percent of cells with lamellipodia for the indicated constructs (right) and the Pearson coefficient of co-localization (PCC) between the indicated constructs and PBD-mRFP-GST (left). Data are presented as mean \pm SEM, $n = 10$. (C) Representative images of cells transfected with RACer and stimulated with ionomycin at 5 min. The original outline of the cell is shown in dashed white lines. (D) Average fold area change of 10 cells expressing RACer and stimulated with ionomycin at 5 min. The data are the mean \pm SEM. (E, F) Representative cells and average fold area change for RACer(T17N). (G, H) The percent cells with an area increase after addition of ionomycin under each of the indicated conditions (G) and the peak fold area change in each case (H). The three conditions labeled as “+ inhibitor” are cells transfected with RACer. The data are the mean \pm SEM, $n = 3$ with at least 10 cells. (I) Representative cells co-expressing PBD-mRFP-GST and RACer or RACer(T17N); “before” denotes before stimulation, and “after” is 10 min after the addition of ionomycin. PCC is calculated as described in Methods. Scale bars are 10 μm throughout.

initiates filopodia outgrowths, which give way to Rac1-dependent lamellipodia based on actin polymerization at the leading edge while RhoA contracts the rear of the cell enabling locomotion. While this model does not capture the complexity of Rho-dependent migration, for example, the contribution of the some 20 “other” Rho GTPases that are not as frequently studied⁸ or the different modes of migration (e.g., mesenchymal and amoeboid),⁹ it has been used to create light-sensitive protein switches that control cell migration.¹⁰ While the reported chimeric proteins have been able to reprogram cells such that they migrate in response to light, light-dependent cellular functions are not ideal for use in large organisms, although PARac has been used to study cell migration in

Drosophila.^{10c} Chemical, mechanical, or physical cues that can penetrate tissue are more appropriate for use in large organisms; however, the existing chimeras cannot be readily altered to respond to chemical or other stimuli because they were developed using specific allosteric or binding interactions between light-sensitive proteins and Rho GTPases.

One cellular messenger pathway that can be reconfigured to respond to different chemical and physical cues is the Ca^{2+} signaling pathway.¹¹ Ca^{2+} is a versatile second messenger that regulates many physiological pathways through Ca^{2+} -responsive proteins and can be regulated by a large “tool-box” of Ca^{2+} -mobilizing proteins. The tool-box of Ca^{2+} -mobilizing proteins can control the cytoplasmic Ca^{2+} concentration in time and

space in response to a variety of chemical cues including neurotransmitters,¹² growth factors,¹³ purines,¹⁴ and physical signals such as light¹⁵ and voltage.¹⁶ Combinations of Ca^{2+} -mobilizing proteins and Ca^{2+} -responsive proteins, each of which have specific isoforms depending on cell type, allow cells to decode Ca^{2+} signals into physiological actions.¹¹ We have shown previously that the Ca^{2+} -responsive protein calmodulin (CaM) and its binding peptides can be used to rationally design protein switches¹⁷ that have specific responses to a variety of chemical and physical cues. In particular, we have engineered a Ca^{2+} -responsive RhoA chimera, named CaRQ,^{17c} that regulates blebbing morphology in a set of epithelial cell lines. While blebbing and amoeboid-like migration have been shown to govern cell locomotion in a number of contexts,¹⁸ we are motivated by developing a migration system for other physiological contexts such as in high-adhesion environments,¹⁹ to complement control over amoeboid-like migration. Our goal is to create a Ca^{2+} -responsive Rac1 chimera that can be used in a variety of cell lines, exploits mesenchymal cell migration, and enables direction-oriented migration toward chemical and light cues.

RESULTS

Conceptual Design of a Rac1-CaM Chimera. Rac1 was rendered sensitive to Ca^{2+} by a fusion of CaM and two of its binding peptides: those from myosin V (IQ2p) and myosin light chain kinase (MLCKp). The IQ2p peptide has moderate, Ca^{2+} -independent affinity for CaM (low micromolar range),²⁰ while the MLCKp peptide has low affinity for apoCaM and very high affinity for Ca^{2+} -CaM (low nanomolar range).²¹ We have previously shown that embedding the IQ2p peptide in the surface-exposed loop between amino acids 49 and 50 of RhoA(Q63L) renders RhoA(Q63L) sensitive to Ca^{2+} -CaM and reasoned that the structural similarity of Rac1 and RhoA would render the analogous chimera (insertion between amino acids 47 and 48) sensitive to Ca^{2+} -CaM.^{17c} We included a tandem amino-terminal fusion of CaM-MLCKp to promote dissociation of CaM from IQ2p upon Ca^{2+} increase (Figure 1A, Supplementary Figure 1). YFP was added as an amino-terminal fusion for visualization. When the YFP-CaM-MLCKp-Rac1(Q61L)/IQ2p chimera was initially expressed in HEK293 cells, there was a strong fluorescent signal from the nucleus (Supplementary Figure 2A). The nuclear localization was greater than typically observed when overexpressing YFP-Rac1(Q61L), and few cells showed lamellipodia; the extra fusion domains likely impaired normal Rac1 export while not interfering with the Rac1 NLS.²² Since our aim was not to create a natively regulated Rac1, but rather a Ca^{2+} -sensitive Rac1, we removed the CAAX motif from the carboxy terminus of Rac1 and added a constitutive membrane localization peptide from Lyn kinase (pLyn) to the amino terminus²³ (Supplementary Figure 2B). Finally, mutations to prevent the chimera from acting as a sink for GAPs (E91H N92H) were introduced^{10a} (Supplementary Figure 2C). We will refer to the full fusion protein pLyn-YFP-CaM-MLCK-Rac1(Q61L E91H N92H Δ CAAX)/IQ2p as RACer for Rac1 activated by Ca^{2+} .

RACer Is a Ca^{2+} -Activated Rac1 Chimera. The RACer chimera had less Rac1 activity at basal Ca^{2+} than Rac1(Q61L) (Figure 1B). Rac1 activity was measured in two ways: by counting the number of cells with lamellipodia on cells expressing YFP, YFP-Rac1(Q61L), RACer and a dominant negative RACer, RACer(T17N) and, in a different cell population, by computing the Pearson correlation coefficient

(PCC) between the localization of these constructs and a probe containing the p21-binding domain (PBD) from p21-activated kinase (PAK)²⁴ (Figure 1B and Supplementary Figures 3 and 4). Using both methods, RACer demonstrated significantly less Rac1 activity than Rac1(Q61L) ($P < 0.001$ by morphology method and $P = 0.032$ by PCC method, $n = 10$ in both cases). There appeared to be more Rac1-like activity of RACer at basal Ca^{2+} by the PCC method than by morphology; this was not concerning since our primary motivation is to regulate morphology and migration.

RACer activation by Ca^{2+} resulted in increased Rac1 activity and morphology changes in cells (Figure 1C–I). We continued to use morphology and PCC analyses to measure Rac1 activity after stimulation by ionomycin, a Ca^{2+} -mobilizing drug. Strictly *in vitro* analyses were not performed because RACer was not well expressed in *E. coli*. Cells expressing RACer and stimulated by ionomycin developed new lamellipodia, and large increases in total area began 2–3 min after the addition of ionomycin and typically lasted for 10–15 min (Figure 1C and D and Supplementary Movies 1 and 2). Rather than reporting the number of lamellipodia per cell or the number of cells with increased lamellipodia formation, the number of cells with an increase in area and the average peak area change are reported. Identifying lamellipodia is subjective, whereas area can be computed with minimal human bias (see Methods for more details). Perfect focus during the imaging time-course was impossible to maintain due to the cell's lamellipodia occupying more than one focal plane after stimulation. Changes in morphology and cell area were not observed when ionomycin was added to cells expressing RACer(T17N), pLyn-YFP alone, or YFP-Rac1(Q61L) alone (Figure 1E–H). Changes in morphology and area were generally insensitive to Y-27632 (Rho kinase inhibitor) and blebbistatin (myosin ATPase inhibitor) although calmidazolium (CDZ, CaM inhibitor) abrogated Ca^{2+} -induced changes (Figure 1G and H). Co-expressing the PBD probe with RACer also prevented Ca^{2+} -induced changes in cell morphology and area; the PCC values with the PBD probe increased by approximately 27.8% with RACer and 4.5% with RACer(T17N) (Figure 1I).

The concentration of free Ca^{2+} needed for RACer to cause an increase in area in 50% of cells, or EC_{50} , was approximately 24 μM (Figure 2). The EC_{50} value was determined by stimulating cells with ionomycin using a CaEGTA- K_2 EGTA buffer to provide reliable concentrations of extracellular free Ca^{2+} . The fit to a standard sigmoid expression was achieved by minimizing the sum of square differences between the data and the model using the three parameters indicated. The quality of the fit, determined by the square of the Pearson coefficient between data and model values, was 0.996, indicating a high-quality fit. For decreasing concentrations of extracellular Ca^{2+} the duration of area increase diminished as shown for representative examples (Figure 2B). The average peak fold area change also decreased as a function of Ca^{2+} concentration, although more as step-function than a sigmoid (Figure 2C). These experiments suggest that there is a strong Ca^{2+} -dependence on the changes in cell morphology and area that have been observed.

RACer mediated Ca^{2+} -dependent morphology changes in a variety of cell types (Figure 3). One motivation for developing a Ca^{2+} -sensitive Rac1 chimera was that our Ca^{2+} -sensitive RhoA chimera caused morphology changes (i.e., bleb formation) only in a set of epithelial-like cell lines (HEK293, HeLa and CHO),^{17c} whereas we believed that a Rac1 chimera could

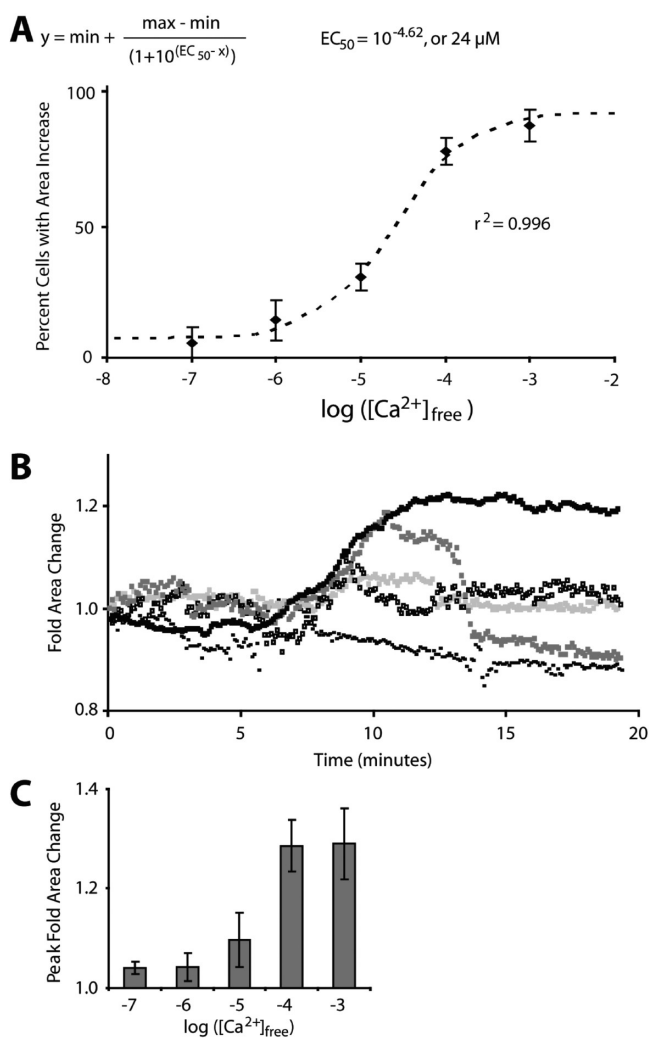


Figure 2. Effect of Ca^{2+} concentration on RACer activation. (A) The percent of cells with an area increase after ionomycin stimulation for the indicated Ca^{2+} concentration in the extracellular buffer (for example, -6 is 10^{-6} M or $1 \mu\text{M}$). The dashed line is the fitted curve using the equation at the top left and the indicated EC_{50} . The data are the mean \pm SEM, $n = 3$ with at least 10 cells. See Methods for more details. (B) Representative fold area data for stimulated single cells corresponding to each Ca^{2+} concentration: black ($1000 \mu\text{M}$), dark gray ($100 \mu\text{M}$), light gray ($10 \mu\text{M}$), open ($1 \mu\text{M}$), dashes ($0.1 \mu\text{M}$). The $1000 \mu\text{M}$ is the average data reproduced from Figure 1D. (C) Peak fold area change for each Ca^{2+} concentration. The data are the mean \pm SEM, $n = 3$ with at least 10 cells.

control morphology in more cell lines since Rac1-dependent lamellipodia formation has been reported in a wide variety of cell types.²⁵ RACer was overexpressed in COS7 (primate fibroblast), RAW264.7 (murine macrophage), and HeLa (human-origen epithelial-like) cells and stimulated with ionomycin as with the above experiments. The response was mostly consistent with our earlier observations: a small, but consistent, area increase was observed in all three cell types. The extent of the area increase was generally less than with HEK293, which is likely a result of the high expression protein expression levels known to occur in HEK293 cells.²⁶ In HeLa cells we noticed filopodia outgrowth in addition to increase in total cell area, which is likely due to the crosstalk between Cdc42 and Rac1 signaling pathways.²⁷ In each case there were significantly fewer cell morphology and area changes with

RACer(T17N) than RACer (Figure 3A) ($P = 0.013, 0.044$, and 0.019 for COS7, RAW264.7, and HeLa cells, respectively). While the RACer-mediated Ca^{2+} -induced changes in these other cell lines were not as extensive as they were in HEK293, taken together they show that RACer has a potentially broad applicability to several cell types, which may be optimized on an application-dependent basis.

RACer Is Robustly Activated by Several Distinct Ca^{2+} -Mobilizing Signals. Engineered systems that utilize Ca^{2+} signaling, such as RACer, can act as modules that can be controlled by distinct Ca^{2+} -mobilizing signals (Figure 4). A remarkable property of Ca^{2+} signaling pathways is that proteins that regulate different stages of Ca^{2+} signaling such as Ca^{2+} mobilization, response, buffering, and removal are combined in different ways in different cell types to achieve complexity and endow Ca^{2+} signals with specificity.¹¹ Therefore it should be possible for a Ca^{2+} -responsive protein, such as RACer, to be activated by some other signal if that signal enables a Ca^{2+} -mobilizing protein to mobilize Ca^{2+} , subject to the spatial and temporal Ca^{2+} needs of the Ca^{2+} -responsive protein, as we have established in other cases previously.^{17a,c} Such a scheme has obvious advantages in the design of therapeutically useful engineered cells; cues to direct the engineered cells may take on a variety of chemical or physical forms depending on the application.

RACer can be activated by at least three stimuli using three classes of Ca^{2+} -mobilizing modules: endogenous, exogenous, and engineered proteins. Adenosine 5'-triphosphate (ATP) binds purinergic receptors on the plasma membrane and causes a brief Ca^{2+} transient via the IP_3 pathway and IP_3R on the endoplasmic reticulum (endogenous).¹⁴ Acetylcholine (ACh) binds to nicotinic ACh-receptor ($\text{nAChR-}\alpha 4$) and opens a Ca^{2+} -permeable pore for a short Ca^{2+} transient, but ACh does not cause a Ca^{2+} -response without $\text{nAChR-}\alpha 4$ in HEK293 cells; however, it can be introduced as a transgene (exogenous).¹² LOVS1K, a recently reported synthetic protein, enables blue light to reversibly activate Orai1 channels, leading to a specific, tunable flux of Ca^{2+} ions when LOVS1K and Orai1 are delivered as transgenes (engineered)¹⁵ (Figure 4A). For each of these three stimuli, cells expressing RACer and the Ca^{2+} -mobilizing protein of interest showed morphological changes and area increases ($P = 0.003, 0.020$, and 0.032 for ATP, ACh, and blue light, respectively) consistent with the Rac1 activation observed with ionomycin (Figure 4B–E and Supplementary Movies 3 and 4). The peak fold area changes were relatively small for the transient-inducing stimuli (ATP and ACh) but were similar between blue light/LOVS1K and ionomycin (Figure 4C). In the case of blue light-activated RACer with LOVS1K, area increase occurred gradually over 20–30 min, which is similar to the reported duration for cytoplasmic Ca^{2+} accumulation due to LOVS1K¹⁵ (Figure 4F). Further, cell area increase stopped and partially reverted after blue light illumination ceased. Similarly, for ACh-activated RACer, the duration of the area increase corresponded to a typical Ca^{2+} transient seen from ACh binding to $\text{nAChR-}\alpha 4$.¹² ATP stimulation also resulted in relatively small changes in cell area, and this was also likely because the ATP-induced Ca^{2+} transient in these cells is short, typically less than 30 s in duration.^{17a} Taking the results of the three stimuli conditions together, this suggests there may be a proportional relationship between the cell area change and the magnitude and/or duration of the Ca^{2+} signal induced by a given stimulus. The ability to activate RACer using exogenous stimuli such as ACh

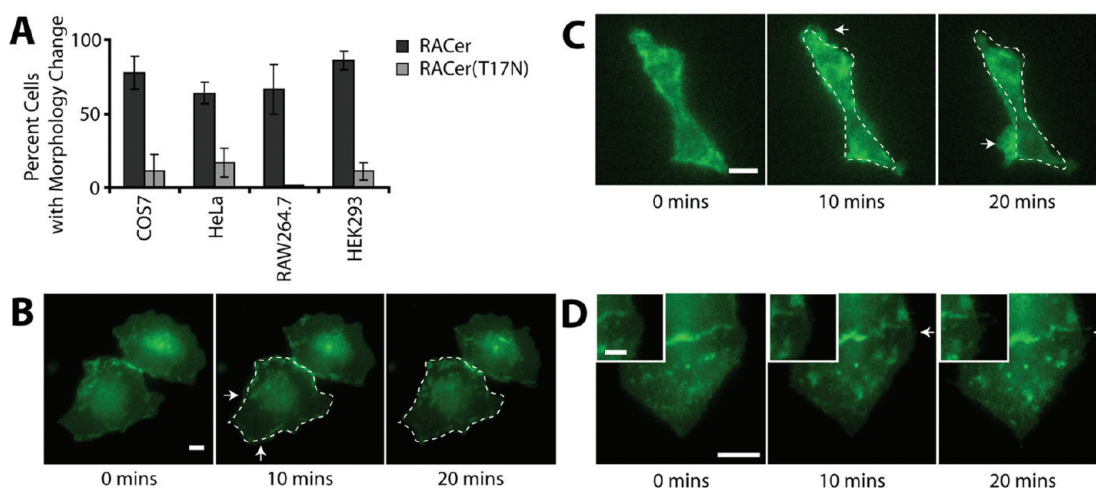


Figure 3. Ca^{2+} stimulation of RACer in several cell lines. (A) Percent of cells with an area increase, or Rac1-like morphology change, after ionomycin stimulation in the indicated cell line for RACer and RACer(T17N). The data are the mean \pm SEM, $n = 3$ with at least 8 cells. (B–D) Representative images of COS7, RAW264.7, and HeLa cells expressing RACer, stimulated with ionomycin at 5 min. White arrows indicate increases/lamellipodia and/or filopodia. Scale bars are 10 μm throughout and 5 μm in the inset.

and blue light show that RACer can be used as a Ca^{2+} -responsive module in combination with potentially many upstream signals.

Directed Cell Migration Mediated by RACer. Prolonged activation of RACer increased cell migration in wound closure and transwell assays (Figures 5 and 6). The role of Rho GTPases in cell migration has been well studied, and Rac1 is known to regulate lamellipodia formation at the leading edge of migrating cells.⁷ We hypothesized that long-term activation of RACer would enhance the migration of HEK293 cells leading to faster penetration and repopulation in a wound closure assay. Cells co-expressing RACer, LOVS1K and Orai1 were illuminated with pulsed blue light (cycling on for 1s, off for 14s) for 24 h resulting in $52.1 \pm 4.6\%$ wound closure (Figure 5). Without illumination, replacing RACer with RACerT17N or illuminating cells without LOVS1K resulted in significantly smaller wound closures of $25.2 \pm 3.7\%$, $17.9 \pm 3.1\%$, and $19.4 \pm 2.0\%$, respectively ($P = 0.011$, 0.007 , and 0.004 , respectively). The myosin ATPase inhibitor blebbistatin also significantly reduced wound closure to $15.8 \pm 6.0\%$ ($P = 0.009$). The Rho kinase inhibitor Y-27632 also appeared to reduce wound closure to $35.8 \pm 3.8\%$, but the difference was not significant ($P = 0.052$). The CaM inhibitor CDZ could not be applied here because we find that cells do not survive 24 h when this inhibitor is present at useful concentrations.

The protein networks used here to increase the migration of cells were delivered by transient transfection, resulting in less than 100% transfection efficiency and a population of cells in the wound assay not expressing RACer (Figure 5B). In wounds that were highly closed, the migrating cells were a mixture of the RACer-expressing and wild type populations, suggesting that the presence of RACer-expressing cells was able to alter the migratory phenotype of neighboring wild type cells. This observation is supported by other reports of migrating cells that can “pull” or “guide” neighboring cells along with them through cell–cell adhesions^{10c} and is also consistent with our earlier work.^{17c}

Engineered cells migrated in response to concentration gradients of VEGF-A, as well as light, in a transwell migration assay (Figure 6). The wound closure assay demonstrated that light could act as a “permissive” signal to induce migration but

did not explicitly provide a directional cue. Further, chemical concentration gradients could not be presented easily using a wound assay. We turned to a transwell migration assay to provide a directional signal for cell migration²⁸ and the ability to present chemicals such as VEGF-A to guide cell migration. Above we showed that ATP- and ACh-induced Ca^{2+} transients initiated lamellipodia formation, and the literature reports of VEGF-A induced VEGFR2 Ca^{2+} transients appear to be a similar shape, amplitude, and duration to ATP and ACh transients.^{17a,c,29} This appeared to be the case in our hands as well (Figure 6A). Cells expressing RACer seeded onto transwell inserts robustly migrated through the porous filters in response to illumination (LOVS1K/Orai co-expression) and 10 ng/mL VEGF-A (VEGFR2 co-expression) (Figure 6B–D). For light/LOVS1K, illumination of RACer significantly increased migration over RACer(T17N), pLyn-YFP, no illumination, or treatment with blebbistatin or Y-27632 ($P = 0.003$, 0.002 , 0.002 , 0.004 , and 0.005 , respectively). For VEGF-A/VEGFR2, results were significant with similar P values. We suspected that ATP and ACh would not be suitable stimulants in this assay because their small molecular size would prevent the porous transwell filter from maintaining an effective chemical concentration gradient, thereby obscuring the cue for cell migration. In experiments where VEGF-A was added to both the apical and basal chambers, cell migration was still significantly different than when VEGF-A was present in only the basal chamber ($P = 0.038$). These experiments show that chemical signals and light can instruct engineered cells to migrate. Further, the directionality of the inducing signal is important to guide cell migration.

A Ca^{2+} -Sensitive Cdc42 Using the RACer Design. The modifications made to Rac1 to create RACer were applied to Cdc42 to create a Ca^{2+} -sensitive Cdc42 chimera (Figure 7). We wanted to test the generalizability of our design with another Rho protein using the same layout of RACer to create a Ca^{2+} -sensitive Cdc42 chimera: pLyn-YFP-CaM-MLCKp-Cdc42-(Q61L E91H N92H Δ CAAX)/IQ2p with IQ2p inserted between amino acids 47 and 48 (Supplementary Figure 5). Cells co-expressing the Cdc42 chimera and the PBD probe from above had a similar extent of co-localization by PCC as with RACer, and after ionomycin stimulation the co-local-

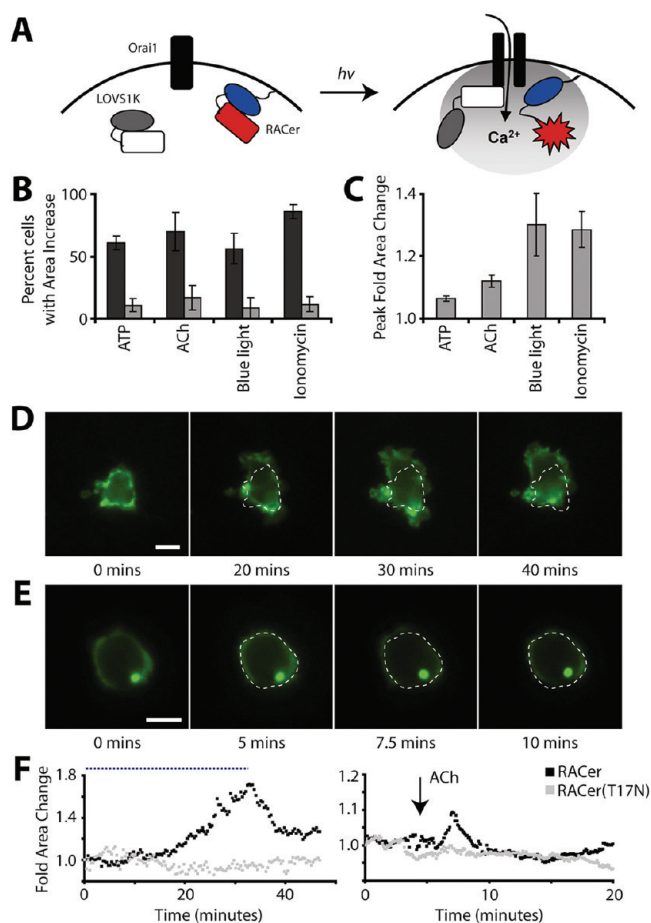


Figure 4. RACer activation by various Ca^{2+} -mobilizing modules. (A) Cartoon of the protein network created by RACer and LOVS1K before and after illumination with blue light. (B, C) Percent cells with area increase expressing RACer or RACer(T17N) (B) or the peak fold area increase (C), stimulated by the indicated chemical. For ATP there was no co-transfection; for ACh, nAChR- $\alpha 4$ was co-transfected; for blue light, LOVS1K and Orail were co-transfected. Ionomycin data are reproduced from Figure 1G for comparison. For panel B, dark bars are RACer and light bars are RACer(T17N). (D, E) Representative images of RACer cells co-transfected with LOVS1K and Orail (D) and nAChR- $\alpha 4$ (E), stimulated with their respective conditions. The dashed line indicates the original cell outline. Scale bars are $10 \mu\text{m}$. (F, G) Fold area changes for RACer cells shown in panels D and E (dark) and corresponding RACer(T17N) cells (light). Duration of periodic illumination is shown by dashed blue line (F) and addition of ACh is indicated by an arrow (G). The data are the mean \pm SEM, $n = 3$ with at least 10 cells.

ization increased 20.8% compared to 3.5% for the T17N dominant negative mutant (Figure 7A). In the absence of the PBD probe, stimulated cells generally developed long, thin filopodia that protruded from the edges of the cell without any particular pattern to their direction (Figure 7B and C and Supplementary Movies 5 and 6). This was not seen with the T17N dominant negative mutant or with the CaM inhibitor CDZ. Y-27632 and blebbistatin had no significant effect on the development of filopodia, as expected given that filopodia generation is not associated with myosin-actin coupling.²⁵ In many cells we noticed that within 2–3 min of filopodia growth, large lamellipodia would develop in their place, which suggests activation of Rac1. Downstream activation of Rac1 by Cdc42 has been reported through the PAK pathway;²⁷ this suggests

that when activated the Cdc42 chimera is able to interact with PAK in addition to regulators of filopodia growth such as WASP.

DISCUSSION

The long-term goal of this work is to develop modular systems to reprogram mammalian cells for useful purposes such as therapeutic platforms or other applications. Specifically, the system presented here enabled cell morphology changes and directed cell migration in response to exogenous stimuli by bringing Rac1 under control of the Ca^{2+} second messenger. In this design, a CaM-binding peptide, IQ2p, with Ca^{2+} -independent CaM affinity, was embedded in a surface-exposed loop of Rac1. A second peptide, MLCKp, with strong, Ca^{2+} -dependent CaM affinity was added to the fusion so that increases in local free Ca^{2+} result in CaM dissociating from IQ2p and associating with the nearby MLCKp. This shows that CaM's ability to recognize target peptides is highly modular, since CaM was able to bind them in the context of a structurally modified chimera.

The inherent modularity of Ca^{2+} signaling was leveraged so that RACer was activated by exogenous stimuli such as ACh and blue light. RACer, a Ca^{2+} -responsive protein, was combined with either nAChR- $\alpha 4$ or LOVS1K, which are Ca^{2+} -mobilizing proteins, to create a multimodule protein network based on Ca^{2+} signaling. These two examples are hardly exhaustive; Ca^{2+} -mobilizing proteins exist that can respond to yellow-red wavelengths of light,³⁰ cytokines and growth factors,¹³ and membrane potential.¹⁶ Existing systems that regulate cell migration in response to exogenous stimuli such as PARac^{10a} and the phytochrome-PIF system^{10b} rely on direct interaction between Rac1 and the stimuli-sensing proteins. This means that these systems cannot be adapted to respond to other stimuli such as biochemical or physical cues. In contrast, RACer is one module that can be combined with other protein modules to sense stimuli, using Ca^{2+} as the intermediary. Input flexibility is a powerful motivation for the further development of synthetic systems based on Ca^{2+} signaling or other modular signaling pathways. Additionally, new insights into Ca^{2+} signaling in nature have been gained: Ca^{2+} can act as a cellular messenger to relay messages between proteins that are foreign to the cellular milieu (here, our chimera and exogenous Ca^{2+} -mobilizing domains). This suggests that Ca^{2+} -based signaling may have been important in the evolution of new cellular pathways.

The Ca^{2+} EC_{50} value of $24 \mu\text{M}$ for RACer was determined by stimulating cells expressing RACer with ionomycin in buffers of different Ca^{2+} concentrations. The output that we considered was the percentage of cells with an increase in cell area indicative of Rac1 activation. Ionomycin treatment of cells results in an equilibrium of extracellular and cytoplasmic Ca^{2+} concentration.³¹ For Ca^{2+} concentrations below $100 \mu\text{M}$, where buffering effects of cellular and extracellular proteins can be significant, a mixture of CaEGTA and K_2EGTA was used to establish buffers with known free Ca^{2+} . The value reported here is similar to the EC_{50} value of $27 \mu\text{M}$ we determined previously for CaRQ.^{17c} Given that the same CaM protein and peptides were used in both chimeras, the similarity between EC_{50} values is not surprising, provided that Rac1 and RhoA have similar binding affinities for their downstream targets and abilities to generate the morphology changes that were used as reporters of chimera activity.

Wound and transwell assays were used to demonstrate that prolonged activation of RACer for 24 h increased the migration

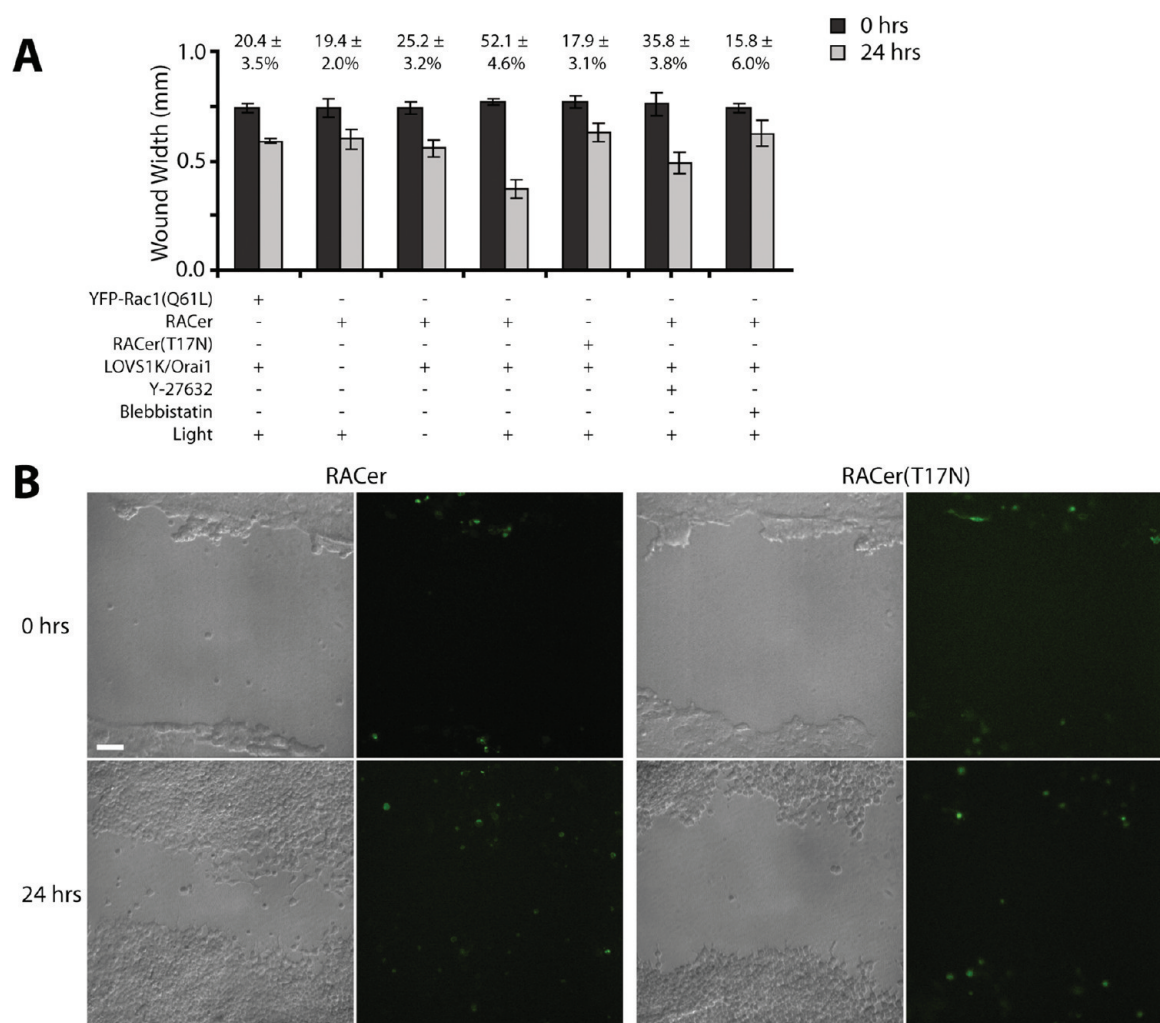


Figure 5. Light-activated cell migration with RACer and LOVS1K. (A) Wound width at 0 h (dark bars) and 24 h (light bars) with percentage change indicated above the bars, for conditions indicated beneath the charts. Data are the mean \pm SEM, $n = 9$ wounds in 3 independent experiments. (B) Representative images of RACer and RACer(T17N) in both YFP and brightfield channels at 0 and 24 h. Scale bar is 100 μ m.

of HEK293 cells. For the wound assays, blue light was used as the stimulus and LOVS1K/Orai1 as the Ca^{2+} -mobilizing module because light can be controlled more easily than chemicals in solution; a continuous stimulus could be provided rather than a bolus dose of ionomycin, ACh, or some other biochemical signal. However, in the transwell assays where a concentration gradient could be maintained for some time a VEGF-A stimulus was used with VEGFR2 as the Ca^{2+} -mobilizing domain to direct cell migration. Overexpression of dominant positive Rho proteins, including Rac1, has usually been noted to suppress cell migration,³² as we have also seen in our wound assay (Figure 5A and B). However, when dominant positive Rac1 is activated with directionality, for example, with PARac, then dominant positive Rac1 can promote cell migration.^{10a,c} A similar phenomenon likely accounts for increased cell migration in these wound assays: periodic activation of RACer via LOVS1K leads to lamellipodia growth in the direction of the wound because this is the only open space available. Growth of lamellipodia into the wound provides a default directionality cue to the cell, enabling migration in that direction and wound closure.

As an extension to the development of RACer and to show that our design strategy is applicable to other Rho family proteins, we created a chimera of Cdc42 analogous to RACer.

The Cdc42 chimera displayed activation kinetics similar to that of RACer, that is, morphology changes could typically be seen in cells 2–3 min after adding ionomycin, and the duration of the morphology change was similar. The morphology change included an initial growth of filopodia followed by lamellipodia in most cells. This suggests that activated Cdc42 was able to interact with PAK, which is known to activate α PIX, a GEF for Rac1.²⁷ Expanding the chimeric Ca^{2+} -control strategy presented here to other Rho family proteins may create insights into the functioning of highly homologous members such as RhoA, RhoB, and RhoC. If the approach is further generalizable, novel control strategies may be possible for other Ras superfamily proteins with diverse functions such as Rab (endosomal shuttling), Ran (nucleocytoplasmic transport), Rap (cell adhesion), and others.

Future work with the RACer construct will further the goal of using it as a functional module for reprogramming cells. The construct may need to be optimized for particular Ca^{2+} -mobilizing signals: for example, using RACer with signals that cause short Ca^{2+} transients such as ACh may require modifications to increase the duration of the Ca^{2+} -mediated cell response. This may be accomplished by changing or mutating the CaM-binding peptides used in RACer or by adding buffering proteins to the vicinity of RACer or the Ca^{2+} -

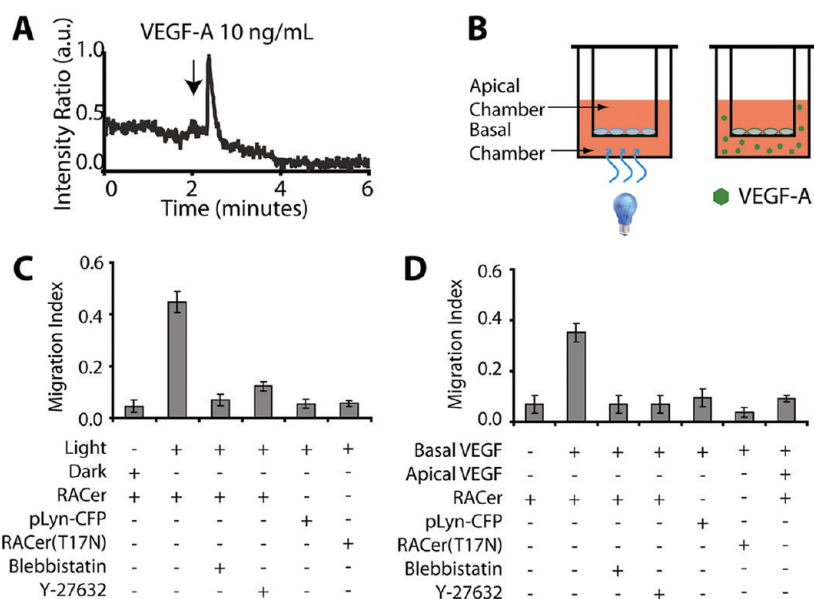


Figure 6. Cell migration along concentration gradients. (A) Ca^{2+} transient in HEK293 cells co-expressing TN-XL Ca^{2+} biosensor and VEGFR2-YFP, stimulated with 10 ng/mL VEGF-A. (B) Cartoon demonstrating the experimental setup for the transwell assays. (C, D) Migration indices for transwell migration assays using light/LOVS1K (C) and VEGF-A/VEGFR2 (D), for the conditions indicated under the data. The migration index is the ratio of the number of cells migrated through the porous filter over 24 h to the total number of cells seeded onto the filter at 0 h (see Supplemental Methods for more detail). The data are the mean \pm SEM for triplicate independent experiments.

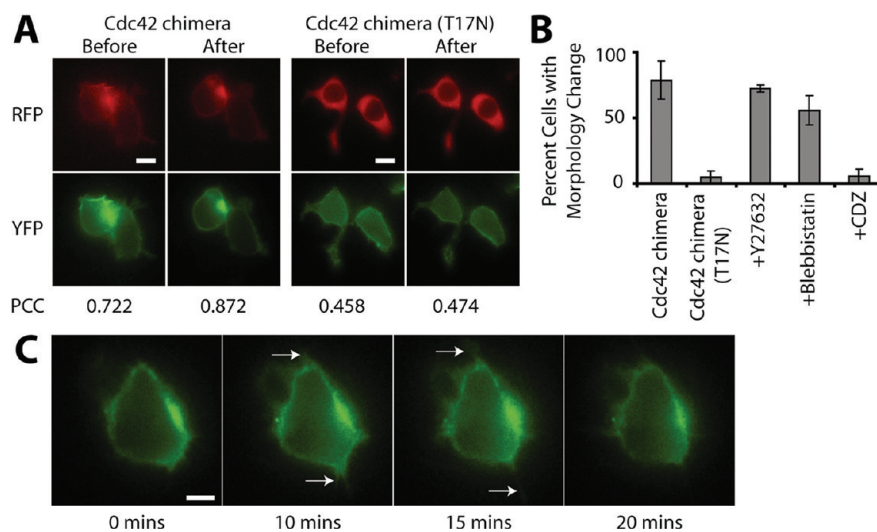


Figure 7. Characterization of a Cdc42-CaM chimera. (A) Representative cells co-expressing PBD-mRFP-GST and Cdc42 chimera or Cdc42(T17N) chimera; “before” denotes before stimulation and “after” is 10 min after the addition of ionomycin. PCC is calculated as described in Methods. (B) Percentage of cells showing filopodia/lamellipodia growth after ionomycin stimulation for the indicated conditions. Conditions labeled as “+ inhibitor” are for cells expressing the Cdc42 chimera. Data are the mean \pm SEM, $n = 3$ with at least 10 cells. (C) Representative images of cells expressing the Cdc42 chimera stimulated with ionomycin at 5 min. White arrows indicate growing filopodia/lamellipodia. Scale bars are 10 μm throughout.

mobilizing module. RACer may also be tested with other protein modules that have been developed to induce cellular apoptosis³³ or promote membrane fusion,³⁴ as first steps toward creating a multifunctional reprogrammed cell. Combining RACer with other Ca^{2+} -mobilizing modules, for example, VEGFR2,¹³ may enable reprogrammed cells to directly migrate toward sources of VEGF *in vitro* and *in vivo* such as areas of active angiogenesis during tumor formation.

Conclusion. We have developed a chimera of Rac1, CaM, and two CaM binding peptides that enabled Rac1-like activity in cell lines when cytoplasmic Ca^{2+} was elevated. The Rac1-CaM chimera, RACer, was used as a Ca^{2+} -responsive module

with a variety of Ca^{2+} -mobilizing protein modules including ATP/purinergic receptors, ACh/nAChR- $\alpha 4$, and blue light/LOVS1K. The combination of RACer and LOVS1K enabled light-sensitive cell migration with repeated activation over 24 h. The development of Ca^{2+} -based synthetic protein networks provides new insights into the role of Ca^{2+} in nature and will ultimately enable mammalian cells to perform complex novel functions that may be of practical therapeutic or industrial value.

METHODS

Plasmid Construction. The RACer plasmid was created with methods described previously.^{17c} Primers used to amplify the amino- and carboxy-terminal fragments of Rac1 and the PBD domain are given in the Supplementary Methods. Plasmids for Rac1, nAChR- $\alpha 4$, Orail, and PBD were Addgene plasmids 13720, 15245, 19756 and 13723, respectively. Mutations to Rac1 (T17N and E91H–N92H) were performed by self-hybridizing PCR; primers are given in the Supplementary Methods.

Cell Culture and Transfection. COS7, HeLa, and HEK293 cells were maintained in Dulbecco's Modified Eagle's Medium supplemented with 10% FBS, 25 mM D-glucose, 1 mM sodium pyruvate, and 4 mM L-glutamine (Invitrogen, Carlsbad, CA) in a T-25 flask. Cells were passaged at 95% confluence using 0.05% trypsin with EDTA (Sigma Aldrich, St. Louis, MO). RAW264.7 cells were maintained in RPMI-1640 supplemented with 10% FBS and 10 mM HEPES. RAW264.7 cells were passaged by cell scraping at 90% confluence. All cell media were supplemented with 100 U/mL penicillin and 100 μ g/mL streptomycin. After passaging, cells were seeded onto glass-bottom dishes at 1:15 dilution. (Mattek, Ashland, MA). Cells were transiently transfected using Lipofectamine 2000 according to manufacturer's directions (Invitrogen).

Reagents Used. Cells were treated with Y-27632 (10 μ M), CDZ (50 μ M), or (–)blebbistatin (10 μ M) by preincubating the inhibitor with cells for 1 h prior to imaging. ATP (10 μ M), ACh (1 mM), and ionomycin (1.5 μ M) were added as a 1:10 dilution directly into the imaging medium. These six chemicals were purchased from Sigma Aldrich. VEGF-A (10 ng/mL), prepared in water, was from Cell Signaling Technology. The Ca²⁺ buffering kit was used according to the manufacturer's directions to establish the indicated extracellular free-Ca²⁺ concentrations (Biotium Inc., Hayward, CA, USA). Rhodamine-phalloidin was used according to the manufacturer's protocol (Invitrogen).

Imaging and Illumination. Imaging was performed using an inverted IX81 microscope with Lambda DG4 xenon lamp source and QuantEM 512SC CCD camera with 40x and 60x oil immersion or 10x objectives (Olympus, Markham, ON, Canada). For LOVS1K, all characterization on the microscope stage (Figure 4 and Movies 3 and 4) received 300 ms pulses of blue light every 10 s. Overnight illumination (Figures 5 and 6) was provided by an iPod programmed to deliver blue light pulses of 1 s on/14 s off; this was the fastest cycling that could be achieved using our method of cycling light on the iPod. The power output of the iPod display (blue screen) was approximately 1 mW/cm².^{17c} The power output of the xenon lamp at the microscope stage is 25 mW/cm². Ca²⁺ transients were recorded using the TN-XL biosensor;³⁵ the data are the ratio of YFP channel intensity to CFP channel intensity when cells were illuminated with CFP excitation light.

Data Analysis. Significance, where discussed, was calculated using the unpaired Student's *t* test without assuming equal variances. The alpha value for this study was set at 0.05, and therefore *P* < 0.05 was considered significant.

For fold area change versus time graphs, cell area was determined using the lowest intensity threshold that captured the whole cell area with ImageJ. For cells that were too close to be delineated automatically, area was calculated by visual inspection. The fold area change was normalized to the cell area

at the outset of an experiment (i.e., the first image in a timelapse experiment always had fold area change = 1). A cell was considered to have an area change if the peak of the fold area change was at least twice the average noise of the graph after the stimulus was added up to 20 min later. The peak fold area change where reported was the global maximum of the fold area change versus time graph. For the Cdc42 chimera experiments, a cell was counted as having a morphology change if filopodia or lamellipodia began growing after the stimulus was added up to 20 min later.

ASSOCIATED CONTENT

Supporting Information

Supplemental figures, methods, and movies. This material is available free of charge via the Internet at <http://pubs.acs.org>.

AUTHOR INFORMATION

Corresponding Author

*Tel: 416-978-7772. Fax: 416-978-4317. E-mail: kevin.truong@utoronto.ca.

Author Contributions

E.M. designed and carried out all experiments and data analysis and wrote the manuscript. E.P. and S.N. created plasmids used in this work. K.T. conceived of the initial idea, provided guidance, and helped write the manuscript.

Notes

The authors declare no competing financial interest.

REFERENCES

- (1) Petros, R. A., and DeSimone, J. M. (2010) Strategies in the design of nanoparticles for therapeutic applications. *Nat. Rev. Drug Discovery* 9 (8), 615–27.
- (2) Breitbach, C. J., Burke, J., Jonker, D., Stephenson, J., Haas, A. R., Chow, L. Q., Nieva, J., Hwang, T. H., Moon, A., Patt, R., Pelusio, A., Le Boeuf, F., Burns, J., Evgin, L., De Silva, N., Cvancic, S., Robertson, T., Je, J. E., Lee, Y. S., Parato, K., Diallo, J. S., Fenster, A., Daneshmand, M., Bell, J. C., and Kirn, D. H. (2011) Intravenous delivery of a multi-mechanistic cancer-targeted oncolytic poxvirus in humans. *Nature* 477 (7362), 99–102.
- (3) Hubbell, J. A., Thomas, S. N., and Swartz, M. A. (2009) Materials engineering for immunomodulation. *Nature* 462 (7272), 449–60.
- (4) Weber, W., and Fussenegger, M. (2009) Engineering of synthetic mammalian gene networks. *Chem. Biol.* 16 (3), 287–97.
- (5) Kalos, M., Levine, B. L., Porter, D. L., Katz, S., Grupp, S. A., Bagg, A., and June, C. H. (2011) T cells with chimeric antigen receptors have potent antitumor effects and can establish memory in patients with advanced Leukemia. *Sci. Transl. Med.* 3 (95), 95–73.
- (6) Kamata, M., Liu, S., Liang, M., Nagaoka, Y., and Chen, I. S. (2010) Generation of human induced pluripotent stem cells bearing an anti-HIV transgene by a lentiviral vector carrying an internal murine leukemia virus promoter. *Hum. Gene Ther.* 21 (11), 1555–67.
- (7) Machacek, M., Hodgson, L., Welch, C., Elliott, H., Pertz, O., Nalbant, P., Abell, A., Johnson, G. L., Hahn, K. M., and Danuser, G. (2009) Coordination of Rho GTPase activities during cell protrusion. *Nature* 461 (7260), 99–103.
- (8) Wheeler, A. P., and Ridley, A. J. (2004) Why three Rho proteins? RhoA, RhoB, RhoC, and cell motility. *Exp. Cell Res.* 301 (1), 43–9.
- (9) Renkawitz, J., Schumann, K., Weber, M., Lammermann, T., Pflücke, H., Piel, M., Polleux, J., Spatz, J. P., and Sixt, M. (2009) Adaptive force transmission in amoeboid cell migration. *Nat. Cell Biol.* 11 (12), 1438–43.
- (10) (a) Wu, Y. I., Frey, D., Lungu, O. I., Jaehrig, A., Schlichting, I., Kuhlman, B., and Hahn, K. M. (2009) A genetically encoded photoactivatable Rac controls the motility of living cells. *Nature* 461 (7260), 104–8. (b) Levskaya, A., Weiner, O. D., Lim, W. A., and

Voigt, C. A. (2009) Spatiotemporal control of cell signalling using a light-switchable protein interaction. *Nature* 461 (7266), 997–1001.

(c) Wang, X., He, L., Wu, Y. I., Hahn, K. M., and Montell, D. J. (2010) Light-mediated activation reveals a key role for Rac in collective guidance of cell movement in vivo. *Nat. Cell Biol.* 12 (6), 591–7.

(11) Berridge, M. J., Lipp, P., and Bootman, M. D. (2000) The versatility and universality of calcium signalling. *Nat. Rev. Mol. Cell Biol.* 1 (1), 11–21.

(12) Nashmi, R., Dickinson, M. E., McKinney, S., Jareb, M., Labarca, C., Fraser, S. E., and Lester, H. A. (2003) Assembly of alpha4beta2 nicotinic acetylcholine receptors assessed with functional fluorescently labeled subunits: effects of localization, trafficking, and nicotine-induced upregulation in clonal mammalian cells and in cultured midbrain neurons. *J. Neurosci.* 23 (37), 11554–67.

(13) Faehling, M., Kroll, J., Fohr, K. J., Fellbrich, G., Mayr, U., Trischler, G., and Waltenberger, J. (2002) Essential role of calcium in vascular endothelial growth factor A-induced signaling: mechanism of the antiangiogenic effect of carboxyamidotriazole. *FASEB J.* 16 (13), 1805–7.

(14) Ralevic, V., and Burnstock, G. (1998) Receptors for purines and pyrimidines. *Pharmacol. Rev.* 50 (3), 413–92.

(15) Pham, E., Mills, E., and Truong, K. (2011) A synthetic photoactivated protein to generate local or global Ca(2+) signals. *Chem. Biol.* 18 (7), 880–90.

(16) Dick, I. E., Tadross, M. R., Liang, H., Tay, L. H., Yang, W., and Yue, D. T. (2008) A modular switch for spatial Ca2+ selectivity in the calmodulin regulation of CaV channels. *Nature* 451 (7180), 830–4.

(17) (a) Mills, E., Pham, E., and Truong, K. (2010) Structure based design of a Ca2+-sensitive RhoA protein that controls cell morphology. *Cell Calcium* 48 (4), 195–201. (b) Mills, E., and Truong, K. (2010) Engineering Ca2+/calmodulin-mediated modulation of protein translocation by overlapping binding and signaling peptide sequences. *Cell Calcium* 47 (4), 369–77. (c) Mills, E., and Truong, K. (2011) Ca(2+)-mediated synthetic biosystems offer protein design versatility, signal specificity, and pathway rewiring. *Chem. Biol.* 18 (12), 1611–9. (d) Mills, E., and Truong, K. (2009) Rate and extent of protein localization is controlled by peptide-binding domain association kinetics and morphology. *Protein Sci.* 18 (6), 1252–60.

(18) (a) Blaser, H., Reichman-Fried, M., Castanon, I., Dumstrei, K., Marlow, F. L., Kawakami, K., Solnica-Krezel, L., Heisenberg, C. P., and Raz, E. (2006) Migration of zebrafish primordial germ cells: a role for myosin contraction and cytoplasmic flow. *Dev. Cell* 11 (5), 613–27. (b) Fackler, O. T., and Grosse, R. (2008) Cell motility through plasma membrane blebbing. *J. Cell Biol.* 181 (6), 879–84. (c) Kardash, E., Reichman-Fried, M., Maitre, J. L., Boldajipour, B., Papisheva, E., Messerschmidt, E. M., Heisenberg, C. P., and Raz, E. (2010) A role for Rho GTPases and cell-cell adhesion in single-cell motility in vivo. *Nat. Cell Biol.* 12 (1), 47–53 ; sup pp 1–11.

(19) Renkawitz, J., and Sixt, M. (2010) Mechanisms of force generation and force transmission during interstitial leukocyte migration. *EMBO Rep.* 11 (10), 744–50.

(20) Trybus, K. M., Gushchin, M. I., Lui, H., Hazelwood, L., Kremensova, E. B., Volkmann, N., and Hanein, D. (2007) Effect of calcium on calmodulin bound to the IQ motifs of myosin V. *J. Biol. Chem.* 282 (32), 23316–25.

(21) Lukas, T. J., Burgess, W. H., Prendergast, F. G., Lau, W., and Watterson, D. M. (1986) Calmodulin binding domains: characterization of a phosphorylation and calmodulin binding site from myosin light chain kinase. *Biochemistry* 25 (6), 1458–64.

(22) Sandrock, K., Bielek, H., Schradi, K., Schmidt, G., and Klugbauer, N. (2010) The nuclear import of the small GTPase Rac1 is mediated by the direct interaction with karyopherin alpha2. *Traffic* 11 (2), 198–209.

(23) Inoue, T., Heo, W. D., Grimley, J. S., Wandless, T. J., and Meyer, T. (2005) An inducible translocation strategy to rapidly activate and inhibit small GTPase signaling pathways. *Nat. Methods* 2 (6), 415–8.

(24) Kraynov, V. S., Chamberlain, C., Bokoch, G. M., Schwartz, M. A., Slabaugh, S., and Hahn, K. M. (2000) Localized Rac activation dynamics visualized in living cells. *Science* 290 (5490), 333–7.

(25) Hall, A. (1998) Rho GTPases and the actin cytoskeleton. *Science* 279 (5350), 509–14.

(26) Thomas, P., and Smart, T. G. (2005) HEK293 cell line: a vehicle for the expression of recombinant proteins. *J. Pharmacol. Toxicol. Methods* 51 (3), 187–200.

(27) Baird, D., Feng, Q., and Cerione, R. A. (2005) The Cool-2/alpha-Pix protein mediates a Cdc42-Rac signaling cascade. *Curr. Biol.* 15 (1), 1–10.

(28) (a) Rosel, D., Brabek, J., Tolde, O., Mierke, C. T., Zitterbart, D. P., Raupach, C., Bicanova, K., Kollmannsberger, P., Pankova, D., Vesely, P., Folk, P., and Fabry, B. (2008) Up-regulation of Rho/ROCK signaling in sarcoma cells drives invasion and increased generation of protrusive forces. *Mol. Cancer Res.* 6 (9), 1410–20. (b) Torika, R., Thuma, F., Herzog, V., and Kirfel, G. (2006) ROCK signaling mediates the adoption of different modes of migration and invasion in human mammary epithelial tumor cells. *Exp. Cell Res.* 312 (19), 3857–71. (c) Worthylylake, R. A., and Burridge, K. (2003) RhoA and ROCK promote migration by limiting membrane protrusions. *J. Biol. Chem.* 278 (15), 13578–84.

(29) Dawson, N. S., Zawieja, D. C., Wu, M. H., and Granger, H. J. (2006) Signaling pathways mediating VEGF165-induced calcium transients and membrane depolarization in human endothelial cells. *FASEB J.* 20 (7), 991–3.

(30) Zhang, F., Prigge, M., Beyriere, F., Tsunoda, S. P., Mattis, J., Yizhar, O., Hegemann, P., and Deisseroth, K. (2008) Red-shifted optogenetic excitation: a tool for fast neural control derived from *Volvox carteri*. *Nat. Neurosci.* 11 (6), 631–3.

(31) Morgan, A. J., and Jacob, R. (1994) Ionomycin enhances Ca2+ influx by stimulating store-regulated cation entry and not by a direct action at the plasma membrane. *Biochem. J.* 300 (Pt 3), 665–72.

(32) (a) Xu, J., Wang, F., Van Keymeulen, A., Herzmark, P., Straight, A., Kelly, K., Takuwa, Y., Sugimoto, N., Mitchison, T., and Bourne, H. R. (2003) Divergent signals and cytoskeletal assemblies regulate self-organizing polarity in neutrophils. *Cell* 114 (2), 201–14. (b) Panopoulos, A., Howell, M., Fotedar, R., and Margolis, R. L. (2011) Glioblastoma motility occurs in the absence of actin polymer. *Mol. Biol. Cell* 22 (13), 2212–20.

(33) Mills, E., Chen, X., Pham, E., Wong, S., and Truong, K. (2011) Engineering a photo-activated caspase-7 for the rapid induction of apoptosis. *ACS Synth. Biol.* 1, 75–82.

(34) Mangeot, P. E., Dollet, S., Girard, M., Ciancia, C., Joly, S., Peschanski, M., and Lotteau, V. (2011) Protein transfer into human cells by VSV-G-induced nanovesicles. *Mol. Ther.* 19 (9), 1656–66.

(35) Mank, M., Reiff, D. F., Heim, N., Friedrich, M. W., Borst, A., and Griesbeck, O. (2006) A FRET-based calcium biosensor with fast signal kinetics and high fluorescence change. *Biophys. J.* 90 (5), 1790–6.